Steady-State Error Suppression and Simplified Implementation of Direct Source Current Control for Matrix Converter with Model Predictive Control

Jiaxing Lei, *Member, IEEE*, Shuang Feng, Patrick Wheeler, *Senior Member, IEEE,* Bo Zhou, Jianfeng Zhao

Abstract- **A matrix converter (MC) with model predictive control (MPC) based on the source reactive power control usually fails to show sinusoidal source currents. The analysis presented in this paper shows that this common combination of converter and control has the inherent inability to suppress some harmonics in the source currents, even with additional passive or active damping control. Direct source current control can be implemented to give sinusoidal source currents and intrinsic active damping. However, the issue of steady-state error in output currents then arises, as the MC topology does not allow of the independent control of source and output currents. Therefore, feedback control of load active power is proposed to address this issue without degrading the fast dynamic performance. Benefiting from the direct source current control, a simplified implementation is also proposed to decrease the number of candidate switching states from 27 to 5, which significantly reduces the computational burden. Experimental results have verified the theoretical analysis and the effectiveness of the proposed control scheme.**

I. INTRODUCTION

[1] The matrix converter (MC) is a direct AC-AC power converter topology without large DC-link energy storage elements [1], as shown in Fig. 1. It has received attentions for four decades [1]-[4]. To generate sinusoidal input and output waveforms, appropriate control methods should be applied to the MC. Linear modulation algorithms such as space vector modulation have been widely adopted for MCs [3], [5]. Yet, they involve complex duty cycle calculation.

In recent years, model predictive control (MPC) has been suggested as a promising alternative to linear modulation algorithms [3], [6]. By taking into account the inherent

J. Lei, S. Feng, and J. Zhao are with the School of Electrical Engineering and with the Jiangsu Provincial Key Laboratory of Smart Grid Technology and Equipment, Southeast University, Nanjing 210096, China, Southeast University, Nanjing 210096, China. (e-mail: jxlei@seu.edu.cn, sfeng@seu.edu.cn, jianfeng_zhao@seu.edu.cn)

P. Wheeler is with the Department of Electrical and Electronics Engineering, University of Nottingham, Nottingham NG7 2RD, U.K. (e-mail: pat.wheeler@nottingham.ac.uk)

B. Zhou is with the Center for More Electric Aircraft Power System, College of Automation Engineering, Nanjing University of Aeronautics and Astronautics, Nanjing 211106, China (e-mail: zhoubo@nuaa.edu.cn).

Color versions of one or more of the figures in this paper are available online at http://ieeexplore.ieee.org.
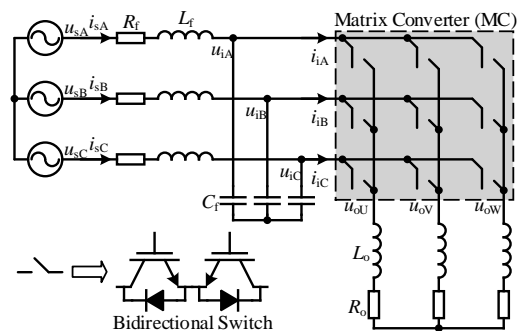
Fig. 1 Basic Schematic of the matrix converter

discrete characteristic of power converters, MPC calculates the cost functions corresponding to all the valid switching states, and then selects the optimal switching state that minimizes the cost function. In every sampling period, MPC only applies the optimal switching state to the MC, without the need of determining duty cycles and the switching sequence which are required by traditional linear modulation schemes. MPC features fast dynamic response and multi-objective optimization, as well as being easy to understand and implement. Hence it has attracted attentions from researchers in various fields of power converters [7], including the MC [3], [6], [8]-[14].

For many MPC schemes developed for MC [8]-[17], source reactive power is the major control objective at the input side, which is realized by including its prediction error in the cost function of MPC. By minimizing the source reactive power, two goals are expected to be achieved. The first goal is ensuring that the source power factor is unity, which can be fully achieved. The second goal is, in coordination with output current control, generating sinusoidal source currents. However, the achievement for the second goal is not perfect in practice. It can be found from the literature [8]-[17] that the actual source currents still contain unwanted harmonics, especially those around the resonant frequency of the input LC filter. Even if additional passive or active damping control methods are applied [16]-[18], source current distortions are still relatively large considering the size of the input filter.

A new MPC scheme was first presented in [19], which applied direct source current control at the input side of MC. The prediction error of source currents instead of reactive power is included in the cost function for this method. The primary goal of this method is to reduce the source current distortion under disturbed input [6], [20]. Experimental results have proved that it always performs much better than the source reactive power control regarding the waveform quality.

Owing to this merit, the idea of this method has been adopted in some newly developed MPC schemes for the MC [21]-[26]. However, due to the active power balance principle, the MC does not allow of independent control of source currents. As a result, the source current reference must be precisely calculated, otherwise there is steady-state error in output currents. Usually, the reference value can be obtained based on the accurate parameters of MC [6], [20]-[25], including the converter efficiency. Yet, accurate parameters (e.g. the efficiency) are hard to obtain, especially under varying working conditions.

In addition to improving waveform quality, the direct source current control also enables reducing the computational burden of MPC. In [26], a simplified MPC with direct source current control was proposed, which was realized by equivalently replacing the prediction errors of source and output currents with those of input currents and output voltages. This method does not need to calculate the predictions of source and output currents, and thus a lot of multiplication operations are saved. However, it considers all the 27 valid switching states when calculating the cost function, which involves many multiplications. Hence, there is still plenty of room to reduce this computational burden.

The concept of "nearest vectors" was proposed in [27] to reduce the number of candidate switching states for MPC. The idea of this simplification has been applied to various converters controlled by MPC [28]-[31], including the MC with the traditional MPC scheme [15]. Nevertheless, all of the existing studies only consider the reduction of output voltage vectors, which is not sufficient for the MPC with direct source current control applied to MC. The input and output circuits of MC are directly coupled and each valid switching state generates an input current vector and an output voltage vector simultaneously. The optimal reduction of candidate switching states should consider the current vectors, voltage vectors and their combinations. Hence the principle and implementation cannot be intuitively extended from existing studies to achieve the minimum number of candidate switching states for the MPC with direct source current control.

This paper firstly presents an explanation of why the traditional MPC with source reactive power control and output current control cannot obtain sinusoidal source currents. It shows that even if the prediction errors of source reactive power and output currents are minimized, source currents could still contain many unwanted harmonics. Besides, additional passive or active damping control cannot completely suppress the harmonics. Therefore, the direct source current control is deemed necessary for the MC with MPC. Secondly, a feedback control method is proposed to suppress the steady-state error of the direct source current control, which is based on regulating the load active power. Finally, a further simplification is proposed for the MPC with direct source current control in order to further reduce the computational burden. The proposed simplification decreases the number of candidate switching states from 27 to 5, thereby reducing the computational burden significantly.

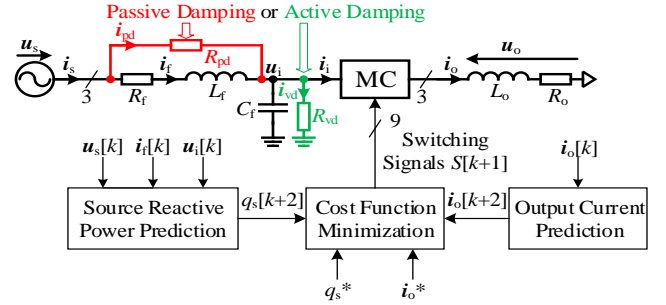The rest of this paper is organized as follows. Section II

Fig. 2 Block diagram of the traditional MPC scheme for MC with source reactive power minimization

analyzes the reason for the inability of traditional modulation schemes to produce sinusoidal source currents. Section III presents the principle of the direct source current control and its side effect, as well as the proposed feedback control method. Section IV introduces the principle and realization of the proposed simplification. Section V presents the experimental verification. Section VI draws the conclusion.

II. MPC WITH SOURCE REACTIVE POWER CONTROL

A. Principle

A general example of traditional MPC schemes with source reactive power control for the MC is shown in Fig. 2. This scheme includes source reactive power prediction, output current prediction, and cost function minimization. To suppress the LC filter resonance, a passive damping resistor can be paralleled to the filter inductor. Alternatively, active damping control can be adopted as studied in [16]-[18], which emulates a virtual resistor at the input of MC via algorithm.

Throughout this paper, the space vector characterizing a three-phase variable is defined as

$$\boldsymbol{x}=x_\alpha + jx_\beta = \frac{2}{3}\left(x_a + x_b e^{j2\pi/3} + x_c e^{j4\pi/3}\right) \tag{1}$$

where vector $\boldsymbol{x}$ represents the voltage vector or current vector at the input side or output side; x_α and x_β are the $\alpha\beta$-axis components of $\boldsymbol{x}$ in two-phase stationary frame; x_a, x_b, and x_c are the components in three-phase stationary frame.

Discrete prediction models are the base of MPC to describe the behavior of the MC system, which have been well developed in literature. The discrete model of the input filter is

$$\begin{bmatrix} \boldsymbol{i}_f[k+1] \\ \boldsymbol{u}_i[k+1] \end{bmatrix} = \boldsymbol{\Phi}_i \begin{bmatrix} \boldsymbol{i}_f[k] \\ \boldsymbol{u}_i[k] \end{bmatrix} + \boldsymbol{\Gamma}_i \begin{bmatrix} \boldsymbol{u}_s[k] \\ \boldsymbol{i}_i[k] \end{bmatrix}, \tag{2}$$

where $\boldsymbol{x}[k]$ represents the value of vector $\boldsymbol{x}$ at the beginning of the kth sampling period; expressions of the matrices $\boldsymbol{\Phi}_i$ and $\boldsymbol{\Gamma}_i$ can be found in [8]. The discrete model to obtain source current is

$$\boldsymbol{i}_s[k] = \boldsymbol{i}_f[k] + \left(\boldsymbol{u}_s[k] - \boldsymbol{u}_i[k]\right)/R_{pd}, \tag{3}$$

where R_{pd} is the passive damping resistance which is infinite if the passive damping control is not applied. The prediction model to obtain the source reactive power is

$$q_s[k] = 1.5\,\mathrm{Im}\left\{\boldsymbol{u}_s[k]\boldsymbol{i}_s^c[k]\right\}, \tag{4}$$

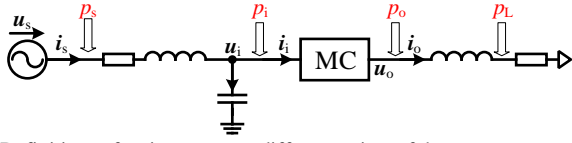where $\mathrm{Im}\{\,\cdot\,\}$ represents the imaginary part of a complex number; superscript c denotes the complex conjugate.

Fig. 3 Definitions of active power at different points of the system

Similarly, the discrete mode for the output circuit is

$$\boldsymbol{i}_{\mathrm{o}}[k+1] = \boldsymbol{\Phi}_{\mathrm{o}}\boldsymbol{i}_{\mathrm{o}}[k] + \boldsymbol{\Gamma}_{\mathrm{o}}\boldsymbol{u}_{\mathrm{o}}[k], \tag{5}$$

Expressions of coefficients $\boldsymbol{\Phi}_{\mathrm{o}}$ and $\boldsymbol{\Gamma}_{\mathrm{o}}$ can also be found in [8].

For a MPC scheme, cost function is the only criterion to determine which switching state is the best to apply to the converter. Usually, it comprises the prediction errors of all the concerning control objectives. For traditional MPC schemes with source reactive power control, the cost function g is

$$g = \lambda_{\mathrm{q}}\left|q_{\mathrm{s}}^{*} - q_{\mathrm{s}}[k+2]\right| + \left|\boldsymbol{i}_{\mathrm{o}}^{*} - \boldsymbol{i}_{\mathrm{o}}[k+2]\right|, \tag{6}$$

where superscript * denotes the reference value. Considering the one sampling period delay caused by the digital control, variables at the beginning of the $(k+2)^{\mathrm{th}}$ rather than the $(k+1)^{\mathrm{th}}$ sampling period should be used for calculations of g. Therefore, the delay compensation needs to be implemented, of which the details are presented in [9]. (6) shows g is the weighted sum of the absolute prediction errors of source reactive power and output currents. Parameter λ_{q} is the weighting factor of source reactive power. Zero g means perfect tracking of output current reference and source reactive power reference, which means output currents are sinusoidal and the input power is pure active. Therefore, the switching state minimizing g should be applied to the MC.

In (6), source reactive power is the only control objective at the input side of the MC. With reference q_{s}^{*} set to zero, it is expected to achieve unit power factor operation. One basic control objective, which is generating sinusoidal source currents, is not directly reflected in (6), but is taken for granted to be achieved based on the instantaneous power theory:

$$\boldsymbol{i}_{\mathrm{s}} = \left(p_{\mathrm{s}} - jq_{\mathrm{s}}\right)\boldsymbol{u}_{\mathrm{s}} / 1.5\left|\boldsymbol{u}_{\mathrm{s}}\right|^{2}, \tag{7}$$

where p_{s} is the source active power. According to (7), in order to obtain sinusoidal source currents, harmonics in both active power p_{s} and reactive power q_{s} should be minimized. For traditional MPC schemes with source reactive power control, harmonics in q_{s} can be directly minimized, but harmonics in p_{s} are indirectly controlled through the output current control. The motivation behind traditional MPC schemes is that p_{s} is determined by the load active power, thereby p_{s} is related to the output current.

However, because of the indirect control of p_{s}, the traditional MPC schemes have the inherent inability to mitigate some harmonics in p_{s} and those harmonics will directly cause distortions in source currents, as analyzed below.

B. Reason for the Source Current Distortions

Fig. 3 shows the definitions of active power at different points of the system, where p_{s} is the source active power generated by the supply, p_{i} is the active power at the input side of MC, p_{o} is the active power at the output side, and p_{L} is the load active power. For the MC, the active power balance principle is that p_{i} is always equal to p_{o} due to the lack of

energy storage elements:

$$p_{\mathrm{i}} = p_{\mathrm{o}}. \tag{8}$$

Nevertheless, p_{s} cannot be considered equal to p_{L} as there are inductors and capacitors on the power transmission path from p_{s} to p_{L}. Dynamic models of the input LC filter and the output inductor have significant effects on the transmission characteristics of harmonics in active power. Unfortunately, traditional MPC schemes ignore these effects, which is the reason why they generate highly distorted source currents.

Expressions of p_{s} and p_{i} are

$$\begin{cases} p_{\mathrm{s}} = \mathrm{Re}\left(1.5\boldsymbol{u}_{\mathrm{s}}\boldsymbol{i}_{\mathrm{s}}^{\mathrm{c}}\right) \\ p_{\mathrm{i}} = \mathrm{Re}\left(1.5\boldsymbol{u}_{\mathrm{i}}\boldsymbol{i}_{\mathrm{i}}^{\mathrm{c}}\right) \approx \mathrm{Re}\left(1.5\boldsymbol{u}_{\mathrm{s}}\boldsymbol{i}_{\mathrm{i}}^{\mathrm{c}}\right) \end{cases}, \tag{9}$$

where $\mathrm{Re}\{\cdot\}$ denotes the real part of a complex number. The approximation sign in (9) is based on the assumption that $\boldsymbol{u}_{\mathrm{i}}$ is approximately equal to $\boldsymbol{u}_{\mathrm{s}}$ if the input filter capacitor is large enough and the ripple of $\boldsymbol{u}_{\mathrm{i}}$ is relatively small. According to Fig. 2, the transfer function $G_{\mathrm{i}}(s)$ from the input current $\boldsymbol{i}_{\mathrm{i}}$ to the source current $\boldsymbol{i}_{\mathrm{s}}$ is

$$G_{\mathrm{i}}\left(s\right) = \frac{\mathcal{L}\left(\boldsymbol{i}_{\mathrm{s}}\right)}{\mathcal{L}\left(\boldsymbol{i}_{\mathrm{i}}\right)} = \frac{L_{\mathrm{f}}s + R_{\mathrm{pd}} + R_{\mathrm{f}}}{R_{\mathrm{pd}}L_{\mathrm{f}}C_{\mathrm{f}}s^{2} + \left(R_{\mathrm{pd}}R_{\mathrm{f}}C_{\mathrm{f}} + L_{\mathrm{f}}\right)s + R_{\mathrm{pd}} + R_{\mathrm{f}}}, \tag{10}$$

where $\mathcal{L}$ represents the Laplace Transform. In (10), $R_{\mathrm{pd}} = +\infty$ corresponds to the case where no damping control is applied. Similarly, with active damping control, $G_{\mathrm{i}}(s)$ is expressed as

$$G_{\mathrm{i}}\left(s\right) = \frac{\mathcal{L}\left(\boldsymbol{i}_{\mathrm{s}}\right)}{\mathcal{L}\left(\boldsymbol{i}_{\mathrm{i}}\right)} = \frac{R_{\mathrm{vd}}}{R_{\mathrm{vd}}L_{\mathrm{f}}C_{\mathrm{f}}s^{2} + \left(R_{\mathrm{vd}}R_{\mathrm{f}}C_{\mathrm{f}} + L_{\mathrm{f}}\right)s + R_{\mathrm{vd}} + R_{\mathrm{f}}}. \tag{11}$$

According to (9), the transfer function from p_{i} to p_{s} can be approximately expressed as

$$\frac{\mathcal{L}\left(p_{\mathrm{s}}\right)}{\mathcal{L}\left(p_{\mathrm{i}}\right)} \approx \frac{\mathcal{L}\left(\boldsymbol{i}_{\mathrm{s}}\right)}{\mathcal{L}\left(\boldsymbol{i}_{\mathrm{i}}\right)} = G_{\mathrm{i}}\left(s\right). \tag{12}$$

It should be noted that (12) is only a rough approximation of the active power transfer function. Accurate derivation of the transfer function should be implemented in the synchronous reference frame which is relatively complicated. (12) is simple but sufficient to explain the effect of the input LC filter.

Analogously, expressions of p_{o} and p_{L} are

$$\begin{cases} p_{\mathrm{o}} = \mathrm{Re}\left(1.5\boldsymbol{u}_{\mathrm{o}}\boldsymbol{i}_{\mathrm{o}}^{\mathrm{c}}\right) \\ p_{\mathrm{L}} = 1.5R_{\mathrm{o}}\boldsymbol{i}_{\mathrm{o}}\boldsymbol{i}_{\mathrm{o}}^{\mathrm{c}} \end{cases}. \tag{13}$$

According to Fig. 2, the transfer function from the output current $\boldsymbol{i}_{\mathrm{o}}$ to the output voltage $\boldsymbol{u}_{\mathrm{o}}$ is

$$G_{\mathrm{o}}\left(s\right) = \frac{\mathcal{L}\left(\boldsymbol{u}_{\mathrm{o}}\right)}{\mathcal{L}\left(\boldsymbol{i}_{\mathrm{o}}\right)} = L_{\mathrm{o}}s + R_{\mathrm{o}}. \tag{14}$$

The approximate transfer function from p_{L} to p_{o} is obtained from (13):

$$\frac{\mathcal{L}\left(p_{\mathrm{o}}\right)}{\mathcal{L}\left(p_{\mathrm{L}}\right)} \approx \frac{\mathcal{L}\left(\boldsymbol{u}_{\mathrm{o}}\right)}{\mathcal{L}\left(\boldsymbol{i}_{\mathrm{o}}\right)R_{\mathrm{o}}} = \frac{G_{\mathrm{o}}\left(s\right)}{R_{\mathrm{o}}}. \tag{15}$$

Based on (8), (12) and (15), the transfer function from load active power p_{L} to source active power p_{s} can be expressed as

$$G_{\mathrm{p}}\left(s\right) = \frac{\mathcal{L}\left(p_{\mathrm{s}}\right)}{\mathcal{L}\left(p_{\mathrm{L}}\right)} = \frac{\mathcal{L}\left(p_{\mathrm{s}}\right)}{\mathcal{L}\left(p_{\mathrm{i}}\right)} \cdot \frac{\mathcal{L}\left(p_{\mathrm{o}}\right)}{\mathcal{L}\left(p_{\mathrm{L}}\right)} = \frac{G_{\mathrm{i}}\left(s\right)G_{\mathrm{o}}\left(s\right)}{R_{\mathrm{o}}}. \tag{16}$$
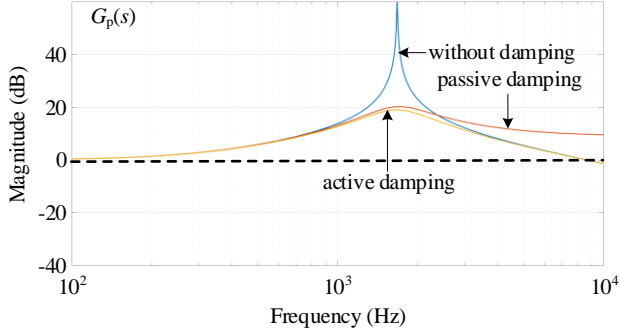
Fig. 4 Frequency responses of the active power transfer function $G_p(s)$. Parameters of the input LC filter and output circuit are the same with those used in experiments. Both the passive damping resistor R_{pd} and the virtual resistor R_{vd} are 19Ω.

It shows that even if the input active power p_i is always equal to the output active power p_o because of the power balance principle, dynamic models of the input LC filter and output circuit have non-negligible effects on the transient relation between source active power p_s and load active power p_L.

For traditional MPC schemes, minimizing the prediction errors of output currents is equivalent to minimizing the harmonics in load active power p_L. Yet, according to (16), only if the magnitude of $G_p(s)$ is larger than 1, the minimized harmonics in p_L could be enlarged and transferred into the source active power p_s. The larger the magnitude of $G_p(s)$ is, the more harmonics p_s will contain. Those enlarged harmonics will be directly reflected in the distortions of source currents.

Frequency responses of $G_p(s)$ with/without passive or active damping control are shown in Fig. 4, from which it can be found that:

1) Without any damping control, the magnitude of $G_p(s)$ at the resonant frequency is larger than 100 (40dB), which means the corresponding harmonics will be amplified 100 times or higher. Therefore, additional damping control is indispensable for traditional MPC schemes.

2) Although the resonance peak could be reduced by the passive or active damping control, it is still up to 20dB. Harmonics around the resonant frequency could be amplified 10 times, which will lead to large distortions in source currents.

3) With passive damping control, the magnitude at high frequencies is about 10dB, which means harmonics at high frequencies can be amplified about 3 times. Considering the rich and widespread harmonics generated by MPC, distortions of source currents are high with the passive damping control.

4) Theoretically, active damping control performs better than the passive one, as it does not increase the magnitude at the high frequencies. If completely realized, it is an acceptable solution to reduce the source current distortions. However, to date, the complete realization of the active damping control for MC with MPC has not been achieved. References [16]-[18] proposed active damping control schemes which modified the dq-axis reference output currents or the load active power with the damping currents extracted from the input voltages. This kind of realization also ignores the effects of dynamic models of input and output circuits, which is less effective than expected to suppress the input filter resonance especially under high resonant frequency. Besides, modifying the output
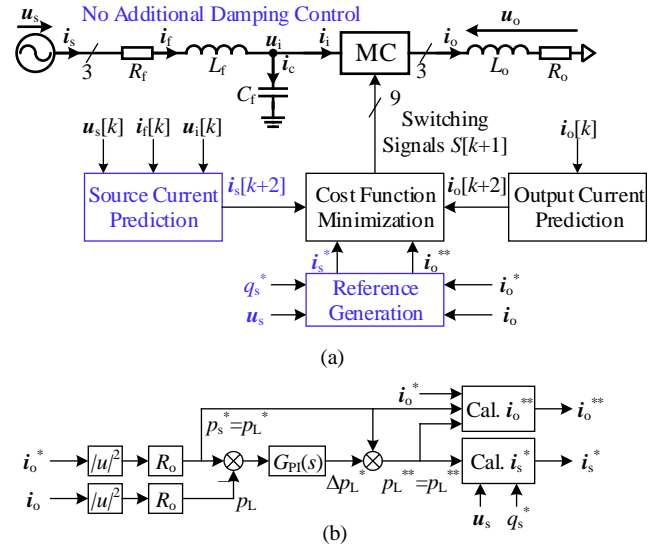

(a)

(b)

Fig. 5 Direct source current control and the proposed feedback control method for the MC with MPC: (a) system control block diagram; (b) proposed feedback control method to regulate the load active power.

reference signals directly affects the output power quality, as the additional damping signals always contain harmonics. As a result, the filter components adopted in [16]-[18] are much larger than the ones in this paper. Actually, the complete realization of the active damping control for MC with MPC relies on modifying the input currents directly, which requires the direct source current control. Yet, as discussed in the next section, the direct source current control does not require additional active damping control, since it has the intrinsic ability to suppress the filter resonance.

To sum up, traditional MPC schemes rely on minimizing the prediction errors of output currents to indirectly control the harmonics in source active power. However, even if the harmonics in output currents (or load active power) are minimized, they can be amplified by the input LC filter and output circuit and transferred into the source active power, causing source current distortions. Especially for harmonics around the resonant frequency of input LC filter, the amplification may be up to 10 times or higher, even if additional passive or active damping control is adopted. This is the reason why traditional MPC schemes theoretically cannot obtain sinusoidal source currents.

III. DIRECT SOURCE CURRENT CONTROL WITH THE PROPOSED FEEDBACK CONTROL METHOD

A. Principle of Direct Source Current Control

To address the issue that traditional MPC schemes with source reactive power control have the inherent inability to obtain high input power quality, direct source current control can be adopted instead, of which the block diagram is shown in Fig. 5(a). Different with the traditional MPC scheme shown in Fig. 2, this scheme includes the source current prediction errors in the cost function:

$$g = \lambda_c \left| \boldsymbol{i}_s^* - \boldsymbol{i}_s [k+2] \right|^2 + \left| \boldsymbol{i}_o^* - \boldsymbol{i}_o [k+2] \right|^2, \qquad (17)$$

where λ_c is the weighting factor of the source current. The

prediction models to calculate source and output currents are the same with those presented in Section II Part A.

(17) shows that g is the weighted square sum of the prediction errors of source and output currents. Zero g means perfect tracking performance for source and output currents. The actual source current is always forced to approach its sinusoidal reference through minimizing the cost function. If one switching state inspires any harmonics or the filter oscillations and further leads to the deviation of the actual source current far from its reference, it will be automatically aborted according to the minimization procedure. Therefore, the direct source current control can directly mitigate source current harmonics and has the intrinsic active damping function, saving additional passive or active damping control. This is a distinct advantage over the traditional MPC schemes.

B. Steady-State Error in the Output Current

According to the active power balance principle of the MC, source currents should be determined by output currents. Though with the above superiority, direct source current control violates this principle to some extent, since it is required to be independent of the output current control. In the multi-objective optimization procedure of MPC, source current control is actually in rivalry with the output current control, subject to the weighting factor λ_s. Therefore, the source current reference i_s^* must be set precisely, otherwise the output control performance would be degraded, e.g. the additional steady-state error in the output current.

Based on the instantaneous power theory, i_s^* can be calculated with

$$i_s^* = \left(p_s^* - jq_s^* \right) u_s / 1.5 \left| u_s \right|^2, \qquad (18)$$

where the reactive power reference q_s^* could be set to 0, so as to achieve unit power factor operation. The reference active power p_s^* is equal to the active power consumed by the load with the converter efficiency η considered.

$$p_s^* = p_L^* / \eta = 1.5 \left| i_o^* \right|^2 R_o / \eta. \qquad (19)$$

In [6], a more accurate model to calculate i_s^* was presented, but it still requires precise system parameters including the efficiency η. In practice, the efficiency is hard to be predetermined since it depends on the system parameters and varies with the working condition. This means the calculation methods in [6] and (18) are both open-loop and will lead to steady-state error in the output current if precise converter efficiency are not obtained. The current error can also be represented by the active power error:

$$p_L = p_s^* - p_d = p_L^* - p_d, \qquad (20)$$

where the error p_d represents the power dissipation, and it can be considered as a DC signal under specific working condition.

It should be noted that the steady-state error is a common issue for MPC. Yet, the error caused by the direct source current control for MC is more obvious and deserves special attention if the imprecise converter efficiency is adopted.

C. Proposed Feedback Control Method

To suppress the steady-state error, this paper proposes a feedback control method, as shown in Fig. 5(b). A PI
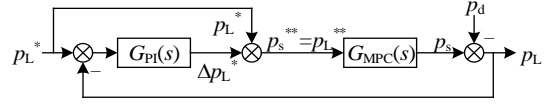

Fig. 6 Control block diagram of the load active power

controller is adopted to regulate the active load power, whose expression is

$$G_{PI}(s) = K_P + K_I / s, \qquad (21)$$

where K_P and K_I are the static gain and integral gain respectively. The output signal of the PI controller is Δp_L^*, which is used to modify the active power reference and further to calculate the source and output current reference:

$$i_s^* = \frac{\left(p_s^{**} - jq_s^* \right) u_s}{1.5 \left| u_s \right|^2} = \frac{\left(p_L^* + \Delta p_L^* - jq_s^* \right) u_s}{1.5 \left| u_s \right|^2}, \qquad (22)$$

$$i_o^{**} = \sqrt{\frac{p_L^{**}}{p_L^*}} i_o^* = \sqrt{1 + \frac{\Delta p_L^*}{p_L^*}} i_o^*, \qquad (23)$$

where p_s^* can be simply set based on (19) with the efficiency assumed as unity. The calculation of the modified output current reference i_o^{**} depends on the load model. If the load is active, the calculation should be changed accordingly.

According to Fig. 5(b), the control block diagram for the load active power is obtained and illustrated in Fig. 6. $G_{MPC}(s)$ is the transfer function from the reference of source active power to the actual value, characterizing the dynamic performance of MPC. As Fig. 6 shows, the proposed method is a closed-loop control method, which considers the active power error p_d as the disturbance. The transfer function from p_d to the actual load active power p_L is obtained from Fig. 6:

$$H(s) = -1 / \left[1 + G_{PI}(s) G_{MPC}(s) \right]. \qquad (24)$$

It is well-known that the PI controller can suppress the effects of a DC disturbance. Therefore, the actual load active power can always reach its reference without steady-state error, so can the output current.

It can be seen from Fig. 5(b) that the amplitude of i_o can always reach its reference at the steady state, no matter the value of R_o is accurate or not. This is because R_o can be considered as an additional static gain of the PI controller, which does not influence the suppression of the effects of a DC disturbance. However, accurate parameters are still preferred for MPC, because MPC relies on the accurate prediction models to describe the converter behavior during each sampling period. The inaccurate parameters will introduce more harmonics in source and output currents.

Although parameters of the introduced PI controller need to be tuned in practice, the tuning effort is relatively small. The PI controller only needs to consider the suppression of the steady-error without too much attention paid to the dynamic performance, since the MPC has very fast dynamic response. Therefore, parameters of the adopted PI controller are applicable in a quite wide range.

IV. SIMPLIFIED IMPLEMENTATION OF THE MPC

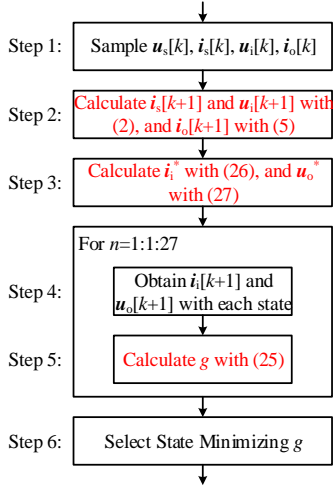In practice, MPC requires a relatively large sampling

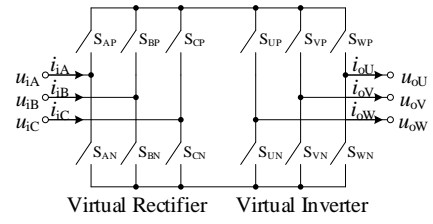Fig. 7. Flowchart of the MPC scheme presented in [26]
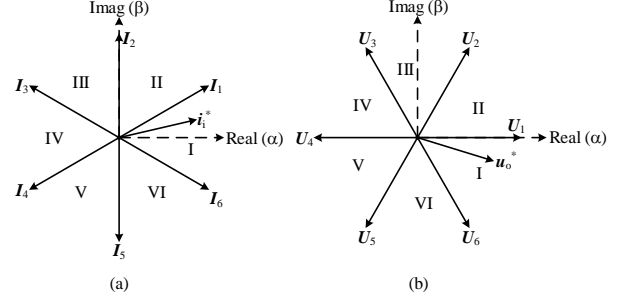

Fig. 8 Equivalent topology of MC

Fig. 9 Distribution of the basic vectors in the complex plain: (a) basic current vectors of the virtual rectifier; (b) basic voltage vectors of the virtual inverter.

frequency to obtain satisfactory waveform quality, which in turn requires all the calculations of MPC must be completed in a small sampling period. According to the principle of the MC, there are 27 valid switching states in total. If all the switching states are considered, the computation burden will be very heavy and thus the sampling frequency cannot be increased. Although the simplified method proposed in [26] has saved a lot of multiplication operations by avoiding the predictions of source and output currents, there is still plenty of room to reduce the involved calculations as it considers all the 27 valid switching states.

Based on the concept of "nearest vectors" in [27]-[31], this paper proposes a further simplification to MPC, which reduces the number of candidate switching states from 27 to only 5. In addition to the reduction of output voltage vectors that has been studied in [27]-[31], the input current vectors are also reduced and the candidate switching states of MC are generated from the combinations of the reduced input current vectors and output voltage vectors.

A. Realization of the Simplified MPC Scheme in [26]

The purpose of the simplified method in [26] is to save as much as possible multiplication operations by avoiding calculating the predictions of source and output currents. With the substitution of (2), (3) where $R_{pd}=+\infty$, and (5) into (17), the cost function can be rewritten as:

$$g = \lambda_c \Gamma_i^2(1,2)\left|i_i^* - i_i[k+1]\right|^2 + \Gamma_o^2\left|u_o^* - u_o[k+1]\right|^2, \quad (25)$$

where i_i^* is the reference input current vector:

$$i_i^* = \frac{i_s^* - \Phi_i(1,1)i_s[k+1] - \Phi_i(1,2)u_i[k+1] - \Gamma_i(1,1)u_s[k+1]}{\Gamma_i(1,2)}, (26)$$

and u_o^* is the reference output voltage vector:

$$u_o^* = \left(i_o^* - \Phi_o i_o[k+1]\right)/\Gamma_o. \quad (27)$$

(17) and (25) are completely equivalent, and hence they can achieve the same control performance. However, (25) does not need to calculate the predictions of source and output currents for every candidate switching state. Therefore, many multiplication operations are saved, reducing the total computational burden.

The flowchart of the method presented in [26] is shown in Fig. 7, which mainly includes 6 steps in one sampling period:
Step 1: Sample the required currents $i_s[k]$, $i_o[k]$ and voltages $u_s[k]$, $u_i[k]$.
Step 2: Implement delay compensation method to calculate $i_s[k+1]$, $i_o[k+1]$, and $u_i[k+1]$. Source voltage $u_s[k+1]$ is obtained through the Lagrange interpolation.
Step 3: Calculate the input current reference i_i^* based on (26) and output voltage reference u_o^* based on (27).
Step 4: Calculate the input current $i_i[k+1]$ and output voltage $u_o[k+1]$ corresponding to each candidate switching state.
Step 5: Calculate the cost function g corresponding to each candidate switching state.
Step 6: Select the switching state that generates the minimum cost function. This state is to be applied to MC in the next sampling period.

As shown in Fig. 7, step 4 and step 5 are repeated 27 times considering all the valid switching states of the MC, which still needs a lot of multiplication operations.

B. Principle of the Proposed Simplification

As it is known in traditional linear modulation methods, the MC can be equalized to a virtual rectifier connected with a virtual inverter [5], which is shown in Fig. 8. Both the rectifier stage and inverter stage generate 6 basic active current or voltage vectors, whose distribution in the complex plain is shown in Fig. 9. The active vectors divide the complex plain into 6 sectors numbered from I to VI. In addition, examples of the reference input current vector i_i^* and output voltage vector u_o^* are also illustrated in Fig. 9, both located in Sector I. Apart from the active vectors, the two stages also generate 3 and 2 zero vectors separately.

The first term at the right side of the equal sign of (25) represents the distance between the actual input current vector i_i and its reference i_i^*. Selecting the switching state that minimizes the cost function is equivalent to finding the basic current vector closest to i_i^*. As shown in Fig. 9(a), if i_i^* is located in sector I, the possible vectors could only be I_6, I_1,
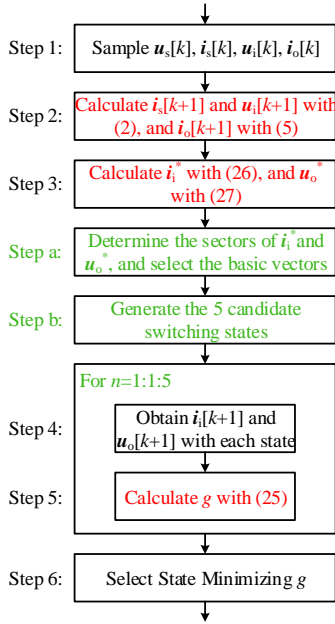
Fig. 10 Flowchart of the proposed simplified MPC

Fig. 11 Picture of the experimental prototype.

V. EXPERIMENTAL VERIFICATION

A. Prototype Parameters

TABLE I Experimental Parameters

Variables	Description	Values
U_s	Source Voltage (L-L RMS)	150 V
f_s	Source Frequency	50 Hz
f_o	Output Frequency	80 Hz
i_{om}^*	Reference Amplitude of Output Current	8 A
L_f	Input Filter Inductor	1.02 mH
C_f	Input Filter Capacitor	8.87 µF
R_f	Resistance of L_f	0.05 Ω
R_d	Passive or Active Damping Resistor	19 Ω
L_o	Output Inductor	4.89 mH
R_o	Output Resistor	10.3 Ω
T_s	Sampling Time	20 µs
λ_q	Weighting Factor of Reactive Power	0.0015
λ_c	Weighting Factor of Source Current	2.4615
K_P	Proportional Gain	0.1
K_I	Integral Gain	200

TABLE II Operation Conditions in Six Experimental Cases

No.	Operation Conditions
1	MPC with source reactive power control and *passive damping control*
2	MPC with source reactive power control and *active damping control*
3	MPC with *direct source current control*
4	MPC with direct source current control and the *proposed feedback control*
5	MPC with direct source current control, the proposed feedback control and *the simplification*
6	MPC with direct source current control, the proposed feedback control and the simplification. *Imprecise parameters* are used in the prediction models.

and the zero vector located at the origin. Therefore, only these vectors need to be considered when calculating the cost function. If i_i^* is located in other sectors, the possible basic vectors can be selected similarly. The second term in (25) represents the distance between the actual output voltage vector u_o and its reference u_o^*. Analogously, only three basic voltage vectors that are closest to u_o^* need to be considered in the cost function calculation.

To sum up, for each stage of the equivalent topology, only three basic vectors (two active vectors and one zero vector) need to be considered in the calculation of cost functions. The pairwise combinations of the two active current vectors and two active voltage vectors generate 4 active vectors of the MC. The combination is based on the topology equivalence [5]. Combining zero vector at one stage with any vector at the other stage generates zero vector of MC. Therefore, there are only 5 candidate switching states in total.

With the proposed simplification, the flowchart of realizing the MPC with direct source current control is shown in Fig. 10. Compared with the method shown in Fig. 7, two additional steps (step a and step b) are inserted after the reference i_i^* and u_o^* are calculated. At step a, sectors of i_i^* and u_o^* are determined and the closest basic vectors are selected accordingly. The sector determination, which is only implemented twice in every sampling period, can be simply obtained by judging the sequence of the three-phase variables. Therefore, the sector determination has minor influence on the computational burden. At step b, the 5 candidate switching states are obtained by combining the basic vectors. In practice, the combination can be stored in a look-up table so as to reduce the execution time. The cost function calculation and minimization only need to consider these 5 states. By comparing Fig. 7 and Fig. 10, it can be found that the repeat times of step 4 and step 5 are reduced from 27 to 5, saving much more multiplication operations.
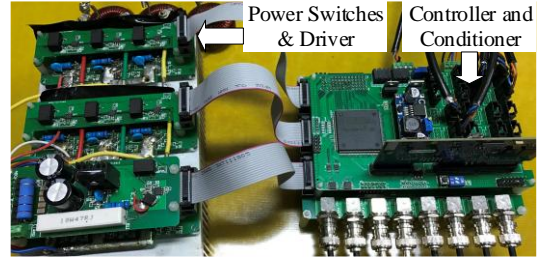
The effectiveness of the theoretical analysis and the proposed improvements to MPC with direct source current control are demonstrated through experiment. A picture of the experimental prototype is shown in Fig. 11. Parameters of the prototype are listed in Table I. The digital controller used is TMS320F28379D which has dual CPU cores operating at 200MHz. Besides, an FPGA is adopted to aid the implementation of the control algorithms, so that all the calculations can be completed within the designed sampling time 20 µs. The input and output performance obtained with MPC is sensitive to the weighting factors. Therefore, for each kind of MPC schemes, experiments are conducted under various values of the weighting factors to find the optimal one that achieves good tradeoff between input and output power quality. The experimental results shown in this section are obtained with the optimal weighting factors listed in Table I. Non-inductance capacitors produced by the EACO company are selected to construct the input LC filter. The passive or active damping resistor is only adopted in traditional MPC
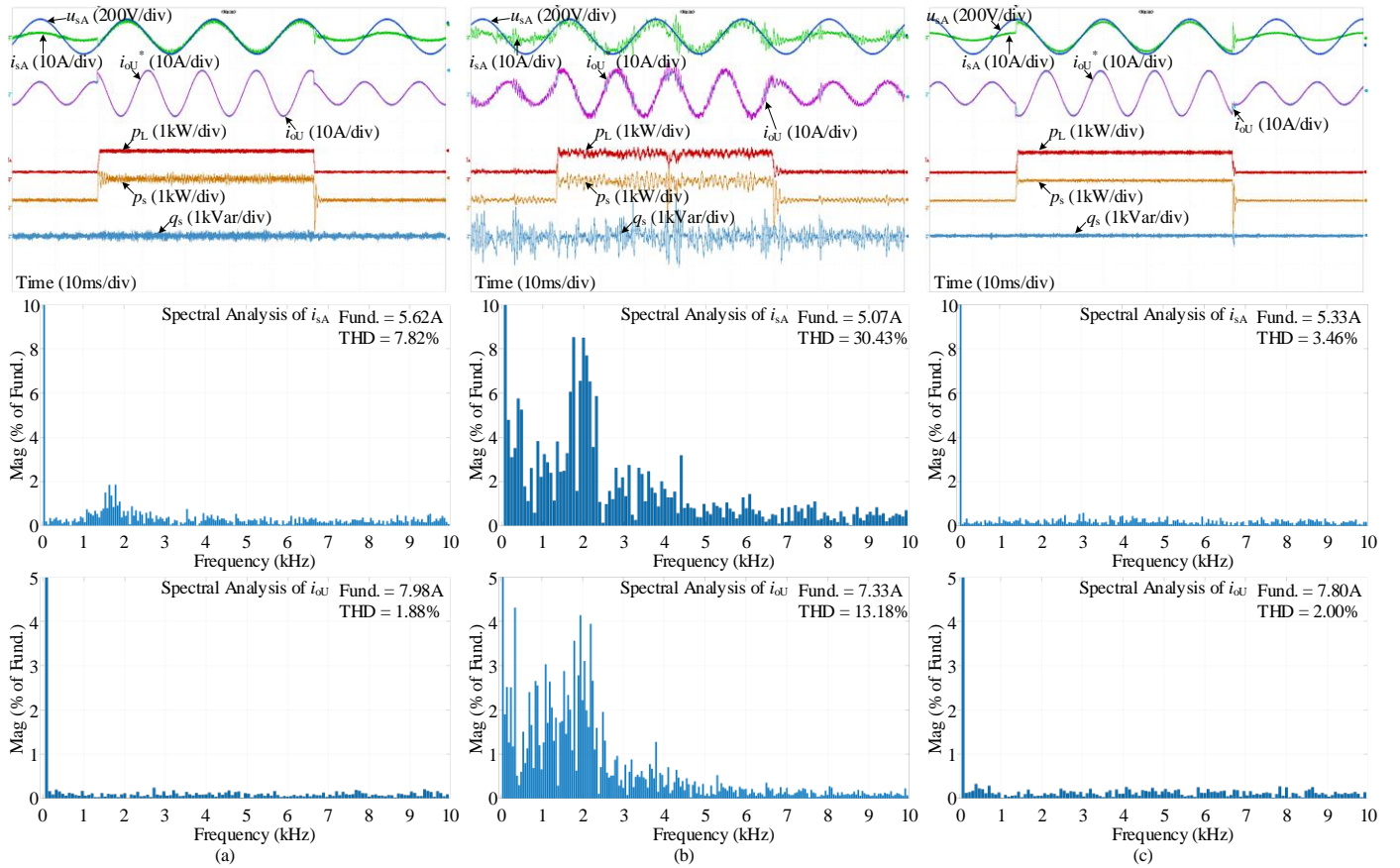
Fig. 12 Experimental results in Case 1 to Case 3: (a) Case 1, the traditional MPC scheme with source reactive power control and with passive damping control; (b) Case 2, the traditional MPC scheme with source reactive power control and with active damping control, the active damping is implemented the same as [16]-[17]; (c) Case 3, the MPC scheme with direct source current control, no additional damping control is applied.

schemes with source reactive power control and is removed in the direct source current control. Parameters of the input and output circuits are obtained using a high accuracy LCR meter.

The experimental verification is conducted in six cases, of which the operation conditions are summarized in Table II. Case 1 and 2 evaluate the performance of the traditional MPC scheme with source reactive power control, where the passive and active damping control are applied separately. Case 3 to Case 5 verify the proposed improvements to the MPC with direct source current control. In Case 6, to evaluate the performance under parameter variations, parameters of the input filter components used in the input prediction model are artificially increased by 5%, while the parameters of the output circuit are reduced by 5%. For simplicity, the converter efficiency considered in Case 3 to Case 6 is fixed at 1, which saves the predetermination of the accurate efficiency without affecting the effectiveness of the verification. When the proposed simplification is applied in Case 5 and Case 6, a look-up table whose dimension is 36×4 is used to store the vector combinations, which only accounts for a minor memory usage of the DSP. To save the space, dynamic performance is evaluated in each case with the reference amplitude of output currents stepping between 8A and 4A, but the spectral analysis is performed at 8A.

B. Experimental Results

Experimental results in Case 1 are shown in Fig. 12 (a). The passive damping control is applied. It can be found that the output current i_{oU} is sinusoidal with THD as low as 1.88%. Besides, the low-frequency ripples of load active power p_L and source reactive power q_s are relatively small. However, it is clear that the source active power p_s is not equal to p_L, but contains significant low-frequency ripples. Consequently, the source current i_{sA} is highly distorted with the total harmonic distortion (THD) up to 7.82%. In particular, i_{sA} contains significant harmonics around the filter resonant frequency ($\approx$1.67 kHz), whose contents are higher than 1.5%. Fig. 12(a) demonstrates that the traditional MPC scheme with source reactive power control has the inability to suppress the harmonics in source currents even with additional passive damping control, which is in good coincidence with the theoretical analysis in Section II Part B.

In Case 2, the active damping control presented in [16]-[17] is applied instead. The reference output currents are modified with the damping currents extracted from the input voltages in the synchronous reference frame. The extraction is based on a high-pass filter. Parameters of this active damping control have been adjusted to obtain the best performance it can reach. Experimental results are shown in Fig. 12(b). Clearly, this kind of active damping control is much less effective than the
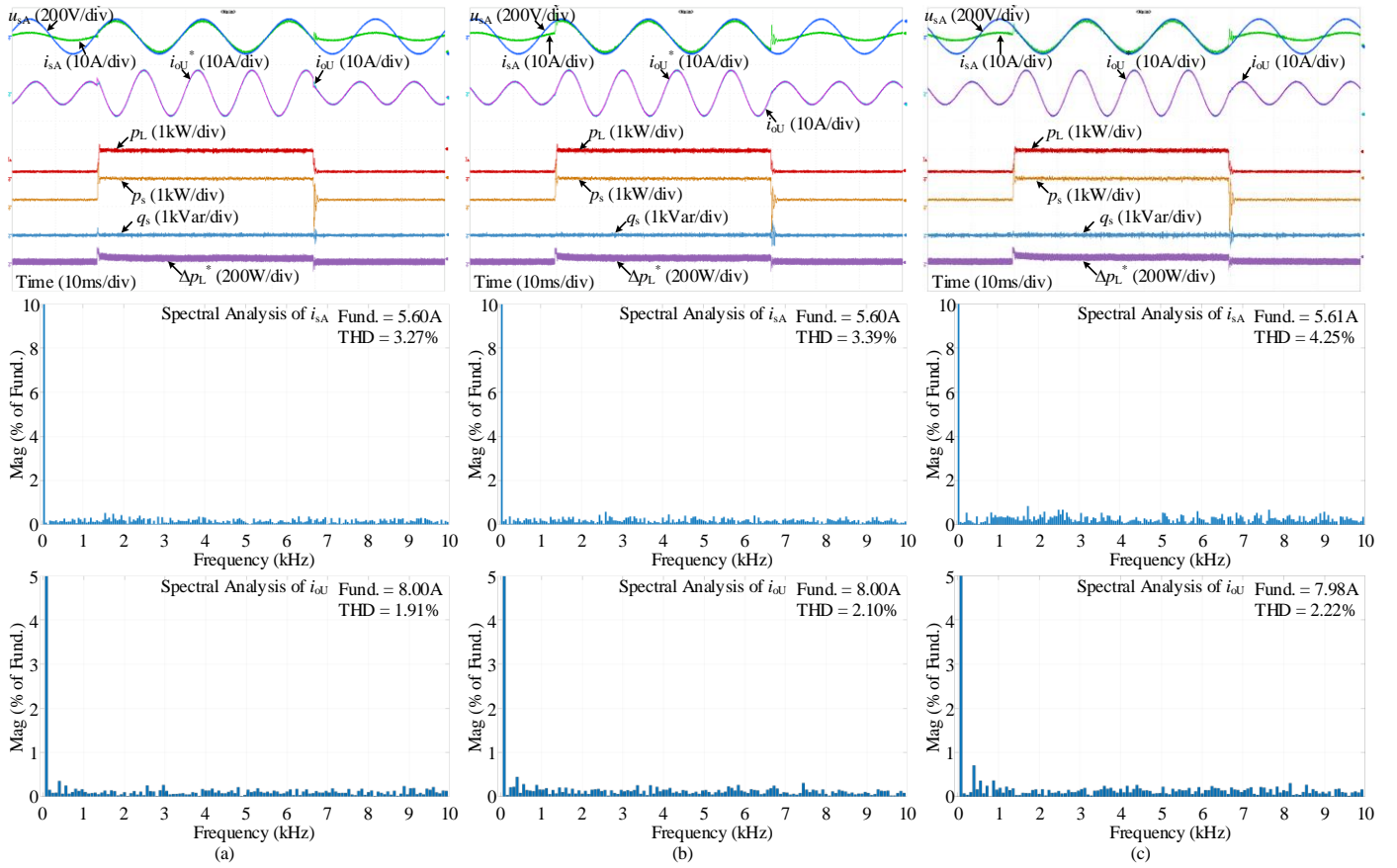
Fig. 13 Experimental results in Case 4 to Case 6, evaluating the direct source current control with the proposed improvements: (a) Case 4, with the proposed feedback control and without the proposed simplification; (b) Case 5, with both the proposed feedback control and simplification; (c) Case 6, with both the proposed feedback control and simplification, parameters in the prediction models are artificially increased by 5% or decreased by 5%.

passive damping control. Both the source and output currents are severely distorted, which is because this kind of realization is incomplete and thus the performance of resonance suppress cannot reach the expectation. It should be noted the damping performance obtained in this case is much worse than that obtained in [16]-[17], for which the reason is that the adopted filter components in this paper are much smaller than those in [16]-[17]. The phenomenon in Fig. 12(b) is also consistent with the discussion in Section II Part B.

Experimental results in Case 3 are shown in Fig. 12(c). The direct source current control is adopted. It can be seen that high quality source current is obtained, with THD reduced to 3.46%. Meanwhile, the output current maintains high power quality with THD around 2.00%. In particular, the source current harmonics around the resonant frequency are suppressed significantly, whose contents are quite small and no larger than others. It should be noted that no additional passive or active damping control is applied in this case. The results prove that the direct source current control could achieve high input and output power quality and has the intrinsic active damping function. Yet, small steady-state error arises with this method. The actual amplitude of output current is 7.80A, less than the reference 8.00A. The steady-state error mainly comes from the imprecise converter efficiency used in (19). It is true that the error can be reduced with precise efficiency. Nevertheless, it is hard to predetermine the

converter efficiency precisely, especially when the operation condition changes.

Then the proposed feedback control is included in Case 4, of which the experimental results are shown in Fig. 13(a). It can be found that the actual amplitude of output current in this case is exactly equal to its reference 8.00A, indicating the suppression of the steady-state error. THDs of source and output currents maintain as low as 3.27% and 2.02% separately. When the reference amplitude of output currents steps, the actual output current can track its reference very fast, just the same as that in Case 3. Therefore, the proposed feedback control strategy can suppress the steady-state error without affecting the power quality and dynamic performance.

The proposed simplification to the MPC with direct source current control is incorporated in Case 5. The experimental results are shown in Fig. 13(b). By comparing Fig. 13(a) and Fig. 13(b), it can be seen that both the steady-state and dynamic performance of the source and output currents in the two cases are almost the same, proving that the proposed simplification does not influence the control performance. However, execution time of the two methods are quite different, as listed in Table III. With the proposed simplification, the execution time is reduced from 19.3 μs to only 10 μs, proving that the proposed simplification could reduce the computational burden significantly. In addition, the average frequencies in the two cases, which are calculated

using the FPGA and listed in Table III, are quite close to each other, indicating that the proposed simplification has little influence on the converter losses.

TABLE III Comparison of the Experimental Results in Case 4 and Case 5

Items	Method in [26]	Proposed
THD of i_o	2.02%	2.09%
THD of i_s	3.27%	3.39%
Average Switching Frequency	10.57 kHz	10.66 kHz
Execution Time	**19.3 μs**	**10.0 μs**

It should be noted that the MPC scheme in Case 4 as well as in Case 3 and Case 6 is implemented in the way presented in [26], which has reduced the computational burden obviously compared with existing studies. Therefore, to the best knowledge of the authors, the proposed simplified MPC scheme is the one requiring minimum computation effort among all of the existing MPC schemes for MC.

In Case 6, performance of the proposed improvements is evaluated considering the parameters in the prediction models increased or decreased by 5%. The experimental results shown in Fig. 13(c) show that THDs of source and output currents are increased slightly to 4.25% and 2.22% respectively, as the result of parameter inaccuracy. Yet, the input and output power quality is still relatively high. In addition, significant reduction of the steady-state error as well as the fast dynamic performance is still achieved in this case. Therefore, the MPC with direct source current control and with the proposed improvements has some robustness to parameter variations.

VI. CONCLUSION

This paper has demonstrated that the traditional MPC scheme has the inherent inability to obtain sinusoidal source currents. Even if an additional damping control is adopted, harmonics around the filter resonant frequency could still be significant in source currents, leading to decreased input power quality. On the contrary, direct source current control directly suppresses the harmonics in source currents and thus features intrinsic active damping function. The output currents maintains good performance meanwhile. From this perspective, the direct source current control should be considered a preferable solution for the MC with a MPC scheme in the future.

A minor side effect of the direct source current control is the steady-state error in the output current if the source current reference is calculated imprecisely. This side effect can be easily suppressed by incorporating a feedback controller. In this paper, PI controller is adopted to regulate the load active power so that zero steady-state error is achieved. In addition, the proposed method also enables the incorporation of resonant controllers to suppress considerable low-frequency harmonics (if any) in output currents.

By extending the concept of "nearest vectors" to MPC with direct source current control, the number of candidate switching states is reduced from 27 to 5. This proposed simplification reduces the computational burden significantly. Therefore, it is possible to achieve better waveform quality with a smaller sampling time if desired. Interestingly, the behavior of MPC with the proposed improvements approaches the traditional linear modulation algorithms.

REFERENCES

[1] J. W. Kolar, T. Friedli, J. Rodriguez and P. W. Wheeler, "Review of Three-Phase PWM AC–AC Converter Topologies," *IEEE Transactions on Industrial Electronics,* vol. 58, no. 11, pp. 4988-5006, Nov. 2011.

[2] L. Empringham, J. W. Kolar, J. Rodriguez, P. W. Wheeler and J. C. Clare, "Technological Issues and Industrial Application of Matrix Converters: A Review," *IEEE Transactions on Industrial Electronics*, vol. 60, no. 10, pp. 4260-4271, Oct. 2013.

[3] J. Rodriguez, M. Rivera, J. W. Kolar and P. W. Wheeler, "A Review of Control and Modulation Methods for Matrix Converters," *IEEE Transactions on Industrial Electronics*, vol. 59, no. 1, pp. 58-70, Jan. 2012.

[4] L. Wang, H. Wang, M. Su, Y. Sun, J. Yang, M. Dong, X. Li, W. Gui and J. Feng, "A Three-Level T-Type Indirect Matrix Converter Based on the Third-Harmonic Injection Technique," *IEEE Journal of Emerging and Selected Topics in Power Electronics*, vol. 5, no. 2, pp. 841-853, June 2017.

[5] L. Huber and D. Borojevic, "Space vector modulated three-phase to three-phase matrix converter with input power factor correction," *IEEE Transactions on Industry Applications*, vol. 31, no. 6, pp. 1234-1246, Nov.-Dec. 1995..

[6] M. Rivera, A. Wilson, C. A. Rojas, J. Rodriguez; J. R. Espinoza, P. W. Wheeler and L. Empringham, "A Comparative Assessment of Model Predictive Current Control and Space Vector Modulation in a Direct Matrix Converter," *IEEE Transactions on Industrial Electronics*, vol. 60, no. 2, pp. 578-588, Feb. 2013.

[7] S. Vazquez, J. I. Leon, L. G. Franquelo, J. Rodriguez, H. A. Young, A. Marquez and P. Zanchetta, "Model Predictive Control: A Review of Its Applications in Power Electronics," *IEEE Industrial Electronics Magazine*, vol. 8, no. 1, pp. 16-31, March 2014.

[8] R. Vargas, J. Rodriguez, U. Ammann and P. W. Wheeler, "Predictive Current Control of an Induction Machine Fed by a Matrix Converter with Reactive Power Control," *IEEE Transactions on Industrial Electronics*, vol. 55, no. 12, pp. 4362-4371, Dec. 2008.

[9] P. Correa, J. Rodriguez, M. Rivera, J. R. Espinoza and J. W. Kolar, "Predictive Control of an Indirect Matrix Converter," *IEEE Transactions on Industrial Electronics*, vol. 56, no. 6, pp. 1847-1853, June 2009.

[10] R. Vargas, J. Rodriguez, C. A. Rojas and M. Rivera, "Predictive Control of an Induction Machine Fed by a Matrix Converter with Increased Efficiency and Reduced Common-Mode Voltage," *IEEE Transactions on Energy Conversion*, vol. 29, no. 2, pp. 473-485, June 2014.

[11] M. López, J. Rodriguez, C. Silva and M. Rivera, "Predictive Torque Control of a Multidrive System Fed by a Dual Indirect Matrix Converter," *IEEE Transactions on Industrial Electronics*, vol. 62, no. 5, pp. 2731-2741, May 2015.

[12] O. Gulbudak and E. Santi, "FPGA-Based Model Predictive Controller for Direct Matrix Converter," in IEEE Transactions on Industrial Electronics, vol. 63, no. 7, pp. 4560-4570, July 2016.

[13] C. F. Garcia, M. E. Rivera, J. R. Rodríguez, P. W. Wheeler and R. S. Peña, "Predictive Current Control with Instantaneous Reactive Power Minimization for a Four-Leg Indirect Matrix Converter," *IEEE Transactions on Industrial Electronics*, vol. 64, no. 2, pp. 922-929, Feb. 2017.

[14] M. B. Shadmand, M. Mosa, R. S. Balog and H. Abu-Rub, "Model Predictive Control of a Capacitorless Matrix Converter-Based STATCOM," *IEEE Journal of Emerging and Selected Topics in Power Electronics*, vol. 5, no. 2, pp. 796-808, June 2017.

[15] M. Siami, D. Arab Khaburi and J. Rodriguez, "Simplified Finite Control Set-Model Predictive Control for Matrix Converter-Fed PMSM Drives," *IEEE Transactions on Power Electronics*, vol. 33, no. 3, pp. 2438-2446, March 2018.

[16] M. Rivera, C. Rojas, J. Rodríguez, P. Wheeler, B. Wu and J. Espinoza, "Predictive Current Control with Input Filter Resonance Mitigation for a Direct Matrix Converter," *IEEE Transactions on Power Electronics*, vol. 26, no. 10, pp. 2794-2803, Oct. 2011.

[17] M. Rivera, J. Rodriguez, B. Wu, J. R. Espinoza and C. A. Rojas, "Current Control for an Indirect Matrix Converter with Filter Resonance Mitigation," *IEEE Transactions on Industrial Electronics*, vol. 59, no. 1, pp. 71-79, Jan. 2012.

[18] J. Lei, B. Zhou, J. Wei, J. Bian, Y. Zhu, J. Yu and Y. Yang, "Predictive Power Control of Matrix Converter with Active Damping Function," *IEEE*

Transactions on Industrial Electronics, vol. 63, no. 7, pp. 4550-4559, July 2016.

[19] M. Rivera, J. Rodriguez, J. R. Espinoza, T. Friedli, J. W. Kolar, A. Wilson, C. A. Rojas, "Imposed Sinusoidal Source and Load Currents for an Indirect Matrix Converter," *IEEE Transactions on Industrial Electronics*, vol. 59, no. 9, pp. 3427-3435, Sept. 2012.

[20] M. Rivera, C. Rojas, J. Rodriguez and J. Espinoza, "Methods of source current reference generation for predictive control in a direct matrix converter," *IET Power Electronics*, vol. 6, no. 5, pp. 894-901, May 2013.

[21] A. Formentini, A. Trentin, M. Marchesoni, P. Zanchetta and P. Wheeler, "Speed Finite Control Set Model Predictive Control of a PMSM Fed by Matrix Converter," *IEEE Transactions on Industrial Electronics*, vol. 62, no. 11, pp. 6786-6796, Nov. 2015.

[22] T. Peng, H. Dan, J. Yang, H. Deng, Q. Zhu, C. Wang, W. Gui, J. M. Guerrero, "Open-Switch Fault Diagnosis and Fault Tolerant for Matrix Converter with Finite Control Set-Model Predictive Control," *IEEE Transactions on Industrial Electronics*, vol. 63, no. 9, pp. 5953-5963, Sept. 2016.

[23] H. Dan, T. Peng, M. Su, H. Deng, Q. Zhu, Z. Zhao and Patrick Wheeler, "Error-Voltage-Based Open-Switch Fault Diagnosis Strategy for Matrix Converters with Model Predictive Control Method," *IEEE Transactions on Industry Applications*, vol. 53, no. 5, pp. 4603-4612, Sept.-Oct. 2017.

[24] G. Zhang, J. Yang, Y. Sun, M. Su, Q. Zhu and F. Blaabjerg, "A Predictive-Control-Based Over-Modulation Method for Conventional Matrix Converters," *IEEE Transactions on Power Electronics*, vol. 33, no. 4, pp. 3631-3643, April 2018.

[25] L. Wang, H. Dan, Y. Zhao, Q. Zhu, T. Peng, Y. Sun and P. Wheeler, "A Finite Control Set Model Predictive Control Method for Matrix Converter with Zero Common-Mode Voltage," *IEEE Journal of Emerging and Selected Topics in Power Electronics*, vol. 6, no. 1, pp. 327-338, March 2018.

[26] M. Siami, M. Amiri, H. K. Savadkuhi, R. Rezavandi and S. Valipour, "Simplified Predictive Torque Control for a PMSM Drive Fed by a Matrix Converter with imposed input current," *IEEE Journal of Emerging and Selected Topics in Power Electronics*, vol. 6, no. 4, pp. 1641-1649, Dec. 2018.

[27] Y. Zhang and H. Lin: "Simplified model predictive current control method of voltage-source inverter", *Proc. of ICPE ECCE, May 2011*, pp. 1726–1733.

[28] K. M. R. Eswar, K. V. P. Kumar and T. V. Kumar, "A simplified predictive torque control scheme for open end winding induction motor drive", *IEEE Journal of Emerging and Selected Topics in Power Electronics*, vol. 7, no. 2, pp. 1162-1172, June 2019.

[29] D. Sun and X. Wang: "Low-complexity model predictive direct power control for DFIG under both balanced and unbalanced grid conditions", *IEEE Transactions on Industrial Electronics*, vol. 63, no. 8, pp. 5186-5196, Aug. 2016.

[30] Z. Gong, P. Dai, X. Yuan, X. Wu and G. Guo, "Design and Experimental Evaluation of Fast Model Predictive Control for Modular Multilevel Converters," *IEEE Transactions on Industrial Electronics*, vol. 63, no. 6, pp. 3845-3856, June 2016.

[31] B. Gutierrez and S. Kwak, "Modular Multilevel Converters (MMCs) Controlled by Model Predictive Control With Reduced Calculation Burden," *IEEE Transactions on Power Electronics*, vol. 33, no. 11, pp. 9176-9187, Nov. 2018.

Jiaxing Lei (S'14-M'17) was born in Dazhou, Sichuan Province, China, in 1991. He received his B.Sc. and Ph.D. degree in electrical engineering from the College of Automation Engineering, Nanjing University of Aeronautics and Astronautics, Nanjing, China, in 2012 and 2017, respectively.

From September 2015 to September 2016, he was a visiting researcher at the Power Electronics, Machines and Control Group (PEMC), University of Nottingham, Nottingham, U.K. In 2017, he joined Southeast University, where he has been a lecturer in the School of Electrical Engineering. His research interest is AC-AC converter, mainly matrix converter, and its application in offshore wind energy system, motor drive system, and et al.

Shuang Feng (M'18) was born in Huaian, Jiangsu Province, China, in 1990. She received her B.Sc. degree in Electrical Engineering from Nanjing University of Aeronautics and Astronautics, Nanjing, China, in 2012. She received her Ph.D. degree in Electrical Engineering from Southeast University, China, in 2017.

She was a visiting researcher in the Department of Electrical and Computer Engineering at Texas A&M University from 2015 to 2016. Since 2017, she has been a lecturer in the School of Electrical Engineering, Southeast University. Her research interests include power system stability and control and data analysis of phasor measurement unit.

Patrick Wheeler (SM'11) received his BEng [Hons] degree in 1990 from the University of Bristol, UK. He received his PhD degree in Electrical Engineering for his work on Matrix Converters from the University of Bristol, UK in 1994.

In 1993 he moved to the University of Nottingham and worked as a research assistant in the Department of Electrical and Electronic Engineering. In 1996 he became a Lecturer in the Power Electronics, Machines and Control Group at the University of Nottingham, UK. Since January 2008 he has been a Full Professor in the same research group. He is currently Head of the Department of Electrical and Electronic Engineering at the University of Nottingham and the Li Dak Sum Chair Professor in Electrical and Aerospace Engineering at the University of Nottingham, China. He is a member of the IEEE PELs AdCom and was an IEEE PELs Distinguished Lecturer from 2013 to 2017. He has published 500 academic publications in leading international conferences and journals.

Bo Zhou was born in Wenzhou, Zhejiang Province, China, in 1961. He received his B.S. degree from Zhejiang University, Hangzhou, China, in 1983, and M.S. degree from Chongqing University, Chongqing, China, in 1986. Then, he worked in Nanjing University of Aeronautics and Astronautics (NUAA), Nanjing, China, where he received his Ph.D. degree in 2000.

He is currently a Professor with the College of Automation Engineering, NUAA, and is the Director of the Jiangsu Key Laboratory of New Energy Generation and Power Conversion. His research interests include power converter, electrical machine driving systems, and renewable power systems.

Prof. Zhou received of the State Technological Invention second-class award in 2009, the Geneva International Invention gold award in 2011 and the Defense Technological Invention first prize in 2008.

Jianfeng Zhao received the B.S. degree in electrical engineering from Huainan Mining Institute, Anhui, China, in 1995, the M.S. degree in automation from Nanjing University of Aeronautics and Astronautics, Nanjing, China, in 1998, and the Ph.D. degree in electrical engineering from Southeast University, Nanjing, China, in 2001.

In 2001, he joined the Faculty of the School of Electrical Engineering, Southeast University, where he has been a Professor since 2008. He has been teaching and researching in the field of high-power electronics and has been serving as the President of the School of Electrical Engineering in Southeast University since 2014. He has authored more than 80 technical papers. He currently holds 35 Chinese patents. His main research interests are utility applications of power electronics in smart grids, such as solid-state transformers, active filters for power conditioning, flexible ac transmission system devices, multilevel ac motor drivers, and efficient energy utilization.

Dr. Zhao has been a member of the Technical Committee of Standard Voltages, Current Ratings and Frequencies of China since 2010. He has also been a member of the All-China Youth Federation since 2010.